Analysis of Zero-Net-Mass-Flux Synthetic Jets using DNS

DECLAN HAYES-McCOY, XI JIANG
School of Engineering and Design
Brunel University
Uxbridge UB8 3PH
ENGLAND
declan.hayes-mccoy@brunel.ac.uk, xi.jiang@brunel.ac.uk

DUNCAN LOCKERBY
School of Engineering
University Warwick
Coventry CV4 7AL
ENGLAND
duncan.lockerby@warwick.ac.uk

Abstract: Axisymmetric direct numerical simulations (DNS) are performed to study the formation criterion and evolution of zero-net-mass-flux synthetic jets. Jet formation is characterised by an oscillating streamwise jet centreline velocity, showing net momentum flux away from the orifice. This momentum flux away from the orifice takes the form of a series of vortical structures, often referred to as a vortex train. Simulation of the jet actuator consists of a modified oscillating velocity profile applied to a wall boundary. The jet issues into quiescent air, and the Reynolds numbers used vary from $85 < Re < 1000$. Variations to the input simulation parameters are carried out in order to determine the overall effects on the flow field. From these results the conditions necessary for the formation of the synthetic jet along with the input parameters that provide an optimal jet output are deduced. Jet optimisation is defined by both the vortical strength and longevity of the vortex train as it travels downstream. This study examines the vortical structures, the jet centreline velocities along with other flow characteristics in order to deduce and visualise the effects of the input parameters on the jet performance. The results attained on altering the oscillation frequency of the jet actuator indicated that synthetic jets with zero mean velocity at the inflow behave significantly differently from jets with non-zero mean velocity at the inflow. An evolution study into the formation of the train of vortical structures associated with the formation of a synthetic jet is performed. This study is accompanied with a time history of the jet centreline velocity, showing the net momentum flux of the fluid away from the orifice of a fully developed synthetic jet. Further details on the jet centreline velocity for all cases are also presented; along with a study on the effect on the vortical structures of altering the Reynolds number of the flow.

Key-Words: Synthetic jet, DNS, axisymmetric, vortical structures

1 Introduction

The ability of jet actuators to alter turbulence production levels and thereby control the turbulence across an aerodynamic surface yields the possibility of skin-friction drag reduction for aerodynamic applications. The successful use of synthetic jet actuators for external flow applications suggests that there are potential aerodynamic gains to be achieved through the use of these devices in a number of internal flow regions, such as ducts and diffusers. Previous experimentation has largely ignored these internal flow applications.

Serpentine engine inlet ducts with a diffuser section introduce significant levels of distortion to the flow into the compressor. Active control of a synthetic jet actuator array could be used to reduce this distortion, mitigate associated unsteadiness and improve the pressure recovery of the diffuser. Amitay & Pitt [1] carried out work into separation control and reattachment in diffusers using synthetic jet actuators, with positive results. This also suggests a possible further role for synthetic jet actuators in reducing the need for larger scale internal flow control devices, such as turning vanes.

This paper computationally analyses the benefits to flow control that can be attained through the use of synthetic jet actuators. The direct numerical simulation (DNS) method used in the analysis allows an accurate capturing of the flow unsteadiness, which is the dominant characteristic of synthetic jets.

2 Synthetic Jet Actuators

Synthetic jet is a zero mass flux device, adding net momentum flux, but no mass flux to its surroundings. Jet formation is defined by Uttukar *et. al.* [2] as a mean outward velocity along the jet axis and corresponds to the clear formation of shed vortices. The layer of vorticity produced by the actuator rolls up to form a vortex ring under its own momentum. The momentum flux away from the orifice is actually a train of vortex pairs or vortex rings being dispersed from the diaphragm during the compression stroke. A pair of these vortices can be seen parallel to each other on either side of the orifice; each equal in magnitude but opposite in direction. Under certain operating conditions a vortex pair (vortex ring in the axisymmetric case) is formed at the orifice edge during the expulsion part of the cycle. This vortex pair or vortex ring is convected away from the orifice.

If the self induced velocity is strong enough this vortex pair or vortex ring is not ingested back into the orifice on the suction part of the cycle. The strength of each vortex shed has been shown by Didden [3] to be related to the flux of vorticity through a (x, y) planar slice of the orifice during the ejection phase of the cycle. Holman & Utturkar [4] determined that jet formation is directly related to the flux of the vorticity from the synthetic jet. The breakdown of the turbulent jet flow tends to occur as a result of spanwise instabilities of the vortex pairs or the streamwise vorticity of the vortex rings.

Depending on the flow symmetry and the repetition rate, the dynamics and interactions of the vortical structures within the pulsed jet can lead to spatial evolution that is remarkably different from the evolution of a continuous jet having the same orifice and time averaged flux of streamwise momentum.

Owing to the suction flow, the time averaged static pressure near the exit plane of a synthetic jet is typically lower than the ambient pressure, and both the streamwise and cross-streamwise velocity components reverse their direction during the actuation cycle. Smith and Glezer [5] defined the time periodic reversal of the flow leads to the formation of a stagnation point on the centreline downstream of the orifice and confines suction flow to a narrow domain near the exit plane.

3 Numerical Methods

Due to the intrinsic unsteady features associated with synthetic jets, typical Reynolds-averaged Navier-Stokes (RANS) methods do not provide sufficient detail to accurately predict the flow and accurately model the vortical structures present. This is due to the inherent time or ensemble averaging of the governing equations by RANS techniques. For this reason DNS is used in this study to resolve all the length and time scales therefore accurately predicting the vortical structures produced by the synthetic jet.

The highly accurate methods of DNS can yield both spatially and temporarily resolved solutions to the Navier-Stokes equations, thus accurately predicting the organised unsteadiness and vortical structures present in the flow. As the motivation behind this study is to determine the formation of the vortical structures produced by a synthetic jet on the onset of turbulence, the accurate flow predictions by a DNS type of simulation are necessary.

The DNS code used for this work has a sixth-order numerical accuracy for the spatial differentiation and third order accuracy for the time advancement [6]. The numerical scheme uses high-order finite difference schemes for the time advancement and spatial discretisation. The time-dependent governing equations are integrated forward in time using a fully explicit low-storage Runge-Kutta scheme. Spatial differentiation is performed by using the high order compact (Padé) finite difference scheme, which is sixth order at its inner points. The points next to the boundary are fourth order and the boundary points themselves are third order, thus the scheme has become known as the Padé 3/4/6 scheme. By applying symmetric conditions to both the primitive variables and their first and second derivatives in the radial direction, the Padé scheme has been extended to achieve the formal sixth order accuracy at the jet centreline, which is the boundary of the computational domain. In the Padé 3/4/6 scheme, the formal sixth order accuracy at the inner points and symmetry boundary is achieved by a compact finite difference differencing. Solutions for the discretised equations are obtained by solving the tridiagonal system of equations. Compared with existing numerical studies, the highly accurate methods employed in this study will be able to more accurately resolve the unsteady vortical structures associated with the flow, which play a predominant role in the turbulence production cycle.

In this study the physical problem considered is a synthetic jet issuing into a wall-bounded domain. The mathematical formulation of the physical problem includes the governing equations for the synthetic jet and the highly accurate numerical solution methods employed to solve the fundamental governing equations, which are described previously [6]. The flow field is described with the compressible time dependent Navier-Stokes equations for the axisymmetric jet. The non-dimensional form of the governing equations is used. Major reference quantities used in the normalisation are the maximum centreline streamwise velocity at the jet nozzle exit (domain inlet), jet nozzle diameter, and the ambient density and viscosity.

There are four boundaries to the computational domain [r: 0-Lr, x: 0-Lx], which represent half of the cross-section of an axisymmetric jet. These are: (1) the symmetric boundary at the jet centreline r = 0. (2) The far side wall boundary in the radial direction r = Lr; (3) an inflow boundary at the domain inlet x = 0, and (4) The wall boundary at the downstream location x = Lx. At the centreline the symmetry conditions are applied. Wall boundary conditions based on the Navier-Stokes characteristic boundary condition formulation [7] are applied at the side boundary in the radial direction and the streamwise directions.

4 Jet Simulation Results

4.1 Simulation details

Several computational cases have been examined; both to determine the simulation parameters required to achieve accurate results and to optimise the jet formation criterion.

Grid refinement studies were carried out, the results of which showed that accurate prediction of the vortical structures required a grid with a total cell count of over 1,000,000 for the axisymmetric simulations. The grid has a uniform distribution in the streamwise direction; however the cell size is sufficiently reduced near the jet shear layer in the radial direction.

As defined by the Courant-Friedrichs-Levy (CFL) condition, in a time-marching simulation the time step must be less than a certain criterion for stability and accuracy considerations. Therefore the CFL number must be sufficiently small to fully resolve the flow features for all actuator frequencies used. In practice the step used should be about one fortieth of the period of the main flow instabilities. In this study, tests with different CFL numbers have been performed and the final CFL number adopted ensures the results are time step independent.

The jet issues into a fixed domain non-dimensionalised by the diameter of the jet orifice. The extent of the computational domain used, is: Lx = 60, Lr = 6.

4.2 Effect of jet frequency

For different pulsating frequencies applied at the inflow, the axisymmetric jet displays significantly different vortical flow structures. As stated by Jiang et al. for non-zero mean velocity jets [6], there is an optimum frequency at which an axisymmetric disturbance receives maximum amplifications in the jet column. Depending on the flow conditions the optimum modes corresponds to a Strouhal number (non-dimensional frequency) in the range St = 0.3 - 0.5, with the most commonly reported number being 0.3. It would be interesting to compare the effects of frequency on the flow field between non-zero mean velocity jets and zero mean velocity synthetic jets. Table 1 gives an outline of all the actuation frequencies for the synthetic jets analysed in this study. The Reynolds number used in the simulations was Re= 500.

Table 1. The computational cases

Designator	Actuator frequency
Case A: ———	St = 0.02
Case B: ---------	St = 0.04
Case C: —·—·—	St = 0.08
Case D: ·····	St = 0.16
Case E: —··—·—	St = 0.40

Figures 1 and 2 show the effect of oscillation frequency on the instantaneous flow characteristics of the zero-net-mass-flux synthetic jets. Figure 1 shows the instantaneous jet centreline velocities at t = 80 for the five cases shown in Table 1, where the line styles used for different computational cases correspond to those described in Table 1. As can be seen in Fig. 1 the centreline streamwise velocities of different cases behave very differently. There are large variations in the velocity profiles, but these variations occur at different locations with different amplitudes. These velocity oscillations are associated with the formation and convection of large-scale vortical structures in the flow field. In the case with the non-dimensional jet frequency of 0.4, no oscillation in the centreline velocity is present.

This is due to re-ingestion of the expelled flow on the return stroke of the jet actuator, before it has travelled a sufficient distance downstream to remain unaffected. In this case the centreline velocity can be noted to drop quickly away from the orifice, with almost no trace of the previous velocity slug remaining.

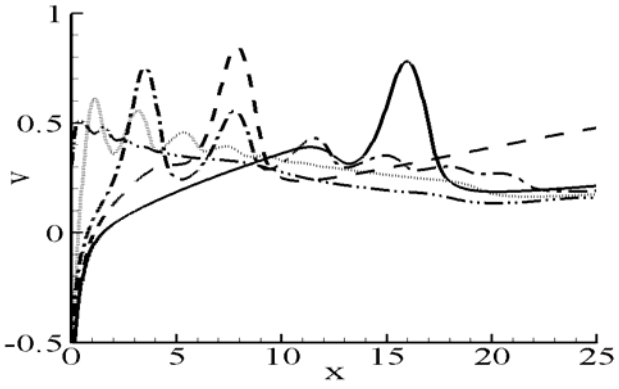

Fig. 1. Jet centreline velocities at t = 80.

Figure 2 shows the instantaneous vorticity contours at t = 80 of cases B, C, D and E. The low frequency cases (St = 0.02 & St = 0.04) do not exhibit true "jet like" characteristics as the oscillation frequency is below the level required to form a vortex train. In these cases only a single vortex or two vortex rings are visible in the flow field; the vortices produced by previous actuator oscillation having completely deteriorated as the actuator completes its successive cycle.

The cases with the actuator frequency of St = 0.08 & St = 0.16 are the only two cases in this study in which a true jet stream is created. It can also be noted that the velocity oscillations for the St = 0.08 case are lower in amplitude and decay more rapidly than the St = 0.04 case, as shown in Fig. 1. This is assumed to be due to partial re-ingestion of the velocity slug with the higher actuator frequency. At a location just beyond x = 10 the streamwise oscillation can be seen to be completely damped out.

The effect of the increased oscillation frequency can also be seen on the vorticity distribution of the jet centreline cross section. The only vortical structures present in the two low frequency cases (f=0.02 & f=0.04) are produced by the previous actuator oscillation. Although the vortical structures of a greater size than those produced by an actuator operating on a higher frequency, the vortical structures do not form a true jet flow. A 'train' of vortical structures can be seen moving downstream in both the St = 0.08 and St = 0.16 cases. However these vortical structures can be seen to degrade and finally disappear by x = 15 for the case with St = 0.08. The lack of any large scale vortical structures can also clearly be noted for the St = 0.4 case.

In Fig. 2, it was seen that larger pulsating frequency leads to smaller scale vortical structures and a corresponding reduction in the streamwise distance between the vortical structures. At higher pulsating frequencies a further reduction in the vortex size occurs, resulting in the rapid deterioration of the vortical structures as they move downstream. This was indeed the case for the simulation with a non-dimensional pulsating frequency of St = 0.4, which has no discernable vortical development downstream.

The important observation in Fig. 2 is that synthetic jet does not display strong vortical structures for the frequency range of Strouhal number St = 0.3 - 0.5, which leads to jet preferred mode of instability for jets with non-zero mean velocity at the domain inlet [6]. For a synthetic jet with zero mean velocity at the inlet, the jet developed significant vortical structures at significantly lower frequencies.

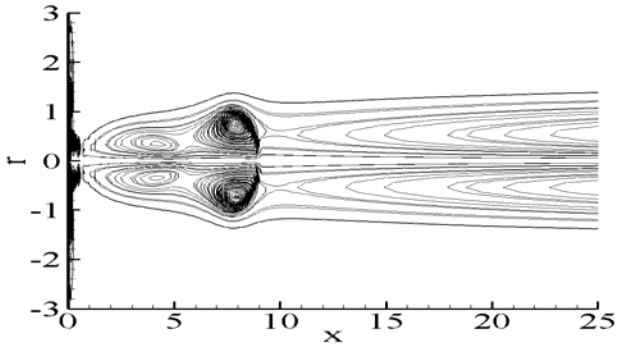

(a) St = 0.04

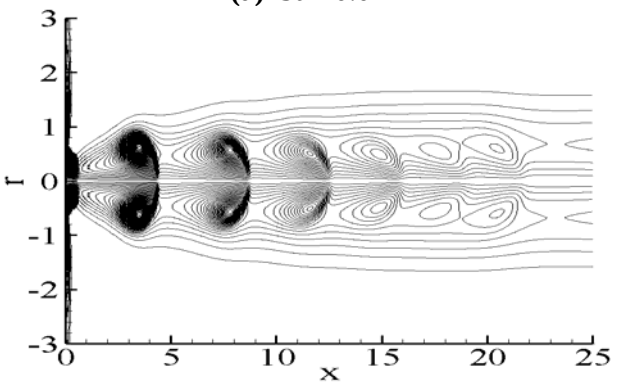

(b) St = 0.08

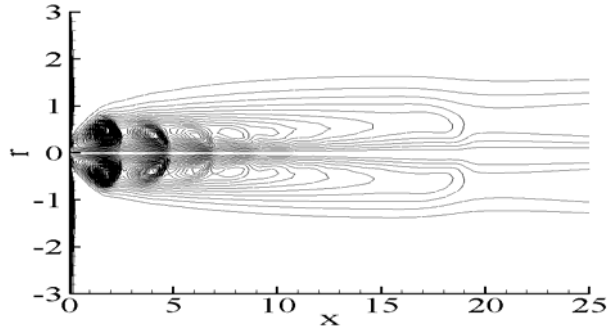

(c) St = 0.16

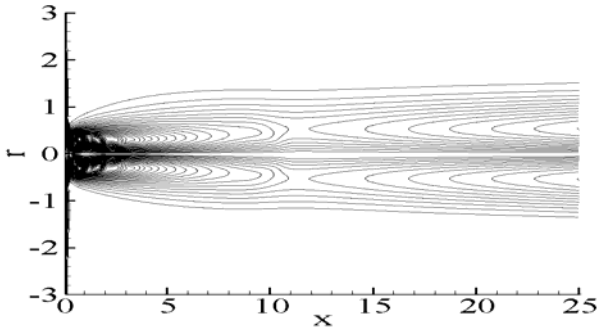

(d) St = 0.40

Fig. 2. Instantaneous vorticity contours at t = 80.

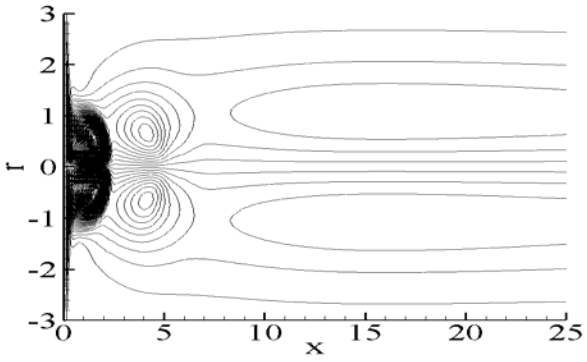

(a) Re = 85

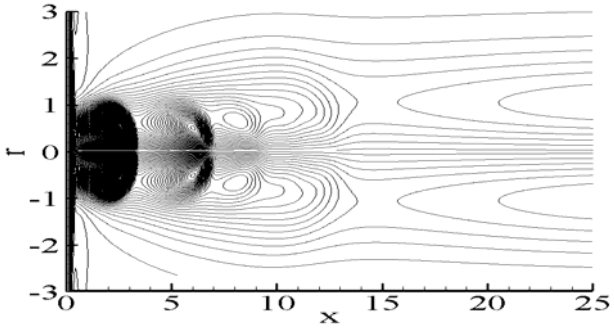

(b) Re = 165

Fig. 3. Effect of Reynolds number: instantaneous vorticity contours at t = 80.

4.3 Effect of Reynolds number

As Reynolds number increases, smaller scales of the flow are visible. In the larger Reynolds number cases there is not as much viscosity present in the flow to dissipate the motions of the small scale eddies. Kinetic energy 'cascades' from large scale eddies to progressively smaller scales until a level is reached for which the scale is small enough for viscous forces become of the order of inertial ones. It is at these small scales where the dissipation of energy by viscous action finally takes place.

Experimentation with varying Reynolds number has a number of implications for determining both the Reynolds number range in which the simulation is valid and the optimum value with respect to maximising vorticity flux. As the Reynolds number decreases the number of grid points required to achieve converged and grid-independent results decreases. Fig. 3 shows the instantaneous vorticity contours at t = 80 at two different Reynolds numbers. In Fig. 3 it can be seen that an increase in Reynolds number leads to an increased intensity and longevity of the vortical structures as they move downstream.

4.4 Jet optimised case

The insights into the effects of the input parameters on the production of a true jet flow were used to create an optimum case in terms of maximum longevity and vortical strength, thereby increasing the turbulent kinetic energy of the flow field and, as shown by Dandois *et. al.* [8], yielding the possibility of separation control and prevention. The parameters used are shown in Table 2.

Figure 4 shows the instantaneous vorticity contours of the optimised case at t = 160. The vortical structures in this case can be seen to gradually reduce in magnitude as they move downstream. It can also be noted that, as the vortex convection speed associated with the streamwise mean velocity only decays slightly downstream, the distance between subsequent vortex centroids does not change significantly. Close comparisons can be made with Fig. 2(b), which uses the same input parameters, but simulated to t = 80. It can be seen that there is no further progression of the vortical structures downstream during the time progression from t = 80-160. The synthetic jet flow can be therefore regarded as statistically or periodically steady during this time interval.

Table 2. Input parameters for the jet optimised case

Jet frequency	0.08
Domain extent (Lx, Lr)	60, 6
Number of cells	1,000,000
Reynolds number	500

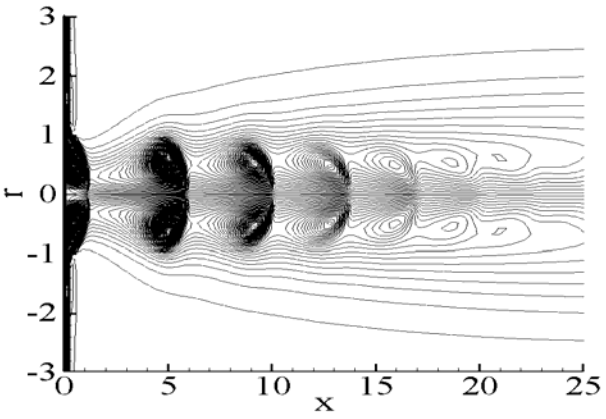

Fig. 4. Jet optimised case at t = 160.

Figure 5 shows the jet centreline velocity within a half actuator cycle of the optimised case, where the line styles used to represent different time instants are described in Table 3. The flow unsteady behaviour is evident in Fig. 5 where the flow changes significantly at locations near the jet nozzle exit but less significantly at the downstream locations. This is mainly because the downstream flow field does not respond quickly to the changes at the inflow, which leads to a net momentum flux away from the orifice of the synthetic jet.

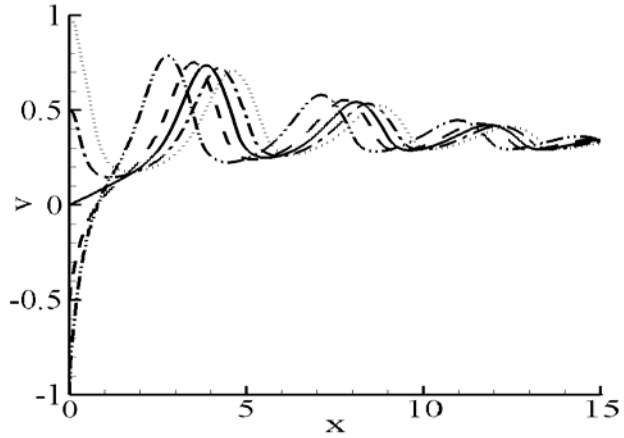

Fig. 5. Instantaneous jet centreline velocity for a half actuator cycle.

Table 3. Velocity profiles for a half actuation cycle

Designator	Time instant
—·—·—	t = 150
---------	t = 152
———	t = 153
—·—·—·	t = 154
·····	t = 156

4.5 Jet evolution

An analysis of the development and evolution of a synthetic jet for the optimum case outlined in section 4.4 at Re = 500 was carried out. For this analysis the simulation was stopped at regular time intervals so that the vorticity distributions and flow structures at the particular time instants could be analysed as they developed. In this case the simulation was stopped at ten unit time intervals between the initial conditions at t = 0 and a time when a train of vortical structures was clearly present, at t = 60. Through this study the formation, convection of each vortical structure associated with the outward expulsion of fluid from the actuator is shown. Corresponding to the jet frequency of St = 0.08, the oscillating velocity profile at the domain inlet has completed about five cycles when the time instant reaches t = 60.

The reduction in vortex intensity as the fluid slug moves downstream is also evident and is shown in a sequence of vorticity distributions in Fig 6. The synthetic jet flow established above the jet exit plane is dominated by the time-periodic formation and advection of discrete vortices as can be seen in Fig. 6. The outward ejection of five slugs of fluid, corresponding to five oscillations of the actuator is presented. From these figures it is clear to see the initial vortex produced after the actuator has been activated is present and beginning to move away from the orifice at t = 20. As can be seen in Fig. 6(a) no discernable vortical structures are present in the flow at t = 10.

In Fig. 6 the initial vortex can be seen to continue to move downstream and is not largely affected by fluid being drawn into the actuator during its suction stroke. As time advances subsequent vortical structures can be seen to be developed by the actuator at each outward ejection phase. Each of these subsequent vortices can be seen to form behind the preceding vortex and to travel downstream with it, keeping a constant distance between vortical cores.

As each vortex moves downstream it can be seen to reduce in intensity as it slowly dissipates. As was shown in Fig. 4 these structures have almost completely dissipated at x = 20 due to mixing with the ambient background fluid [6], and are almost indistinguishable from the background fluid beyond this point. At this point they can be determined to no longer being phased locked with the actuator oscillation [9].

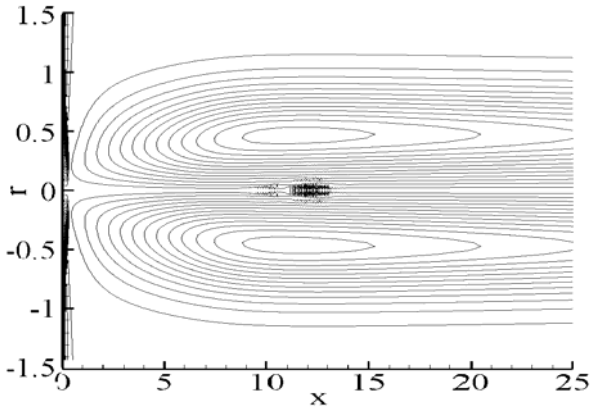

(a) t = 10

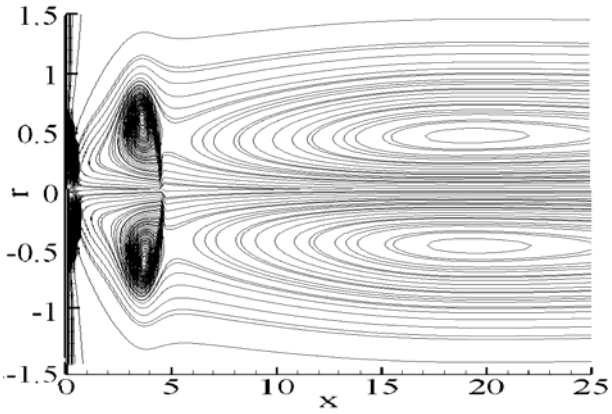

(b) t = 20

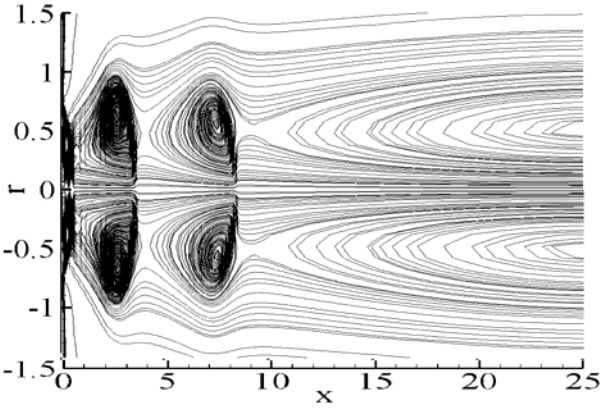

(c) t = 30

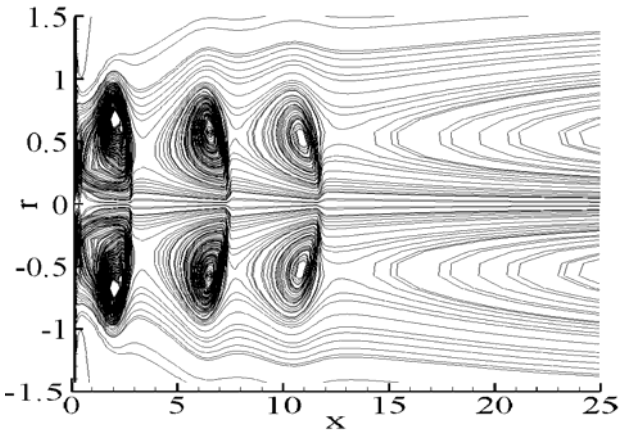

(d) t = 40

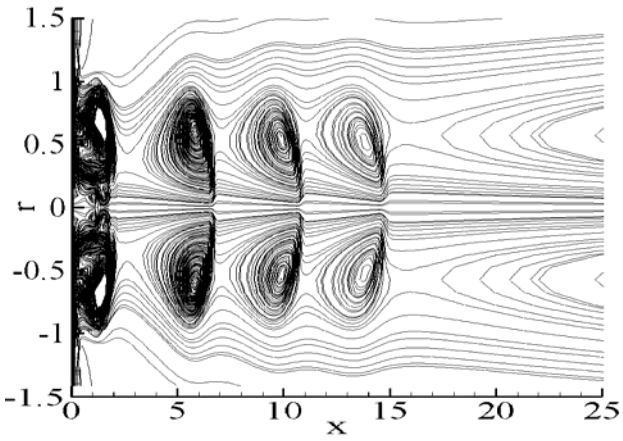

(e) t = 50

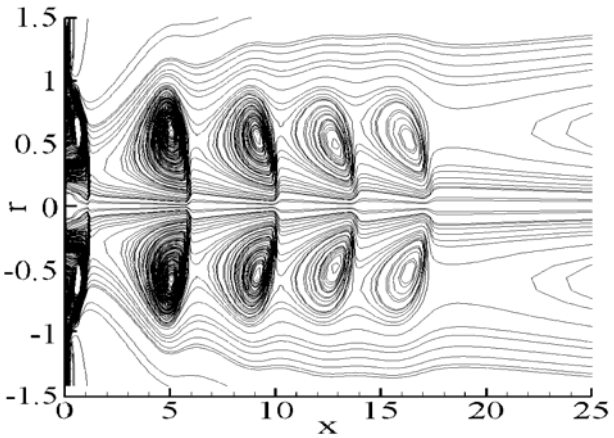

(f) t = 60

Fig.6 Time evolution of the vortical structures of the optimised case.

4.6 Jet centreline velocity history

To further indicate the periodic behavior of the flow field at a later stage when the flow is fully developed, Fig. 7 shows the centreline velocity history of this case after t = 80, for two locations x = 0 and x = 15 respectively. The periodic variation at the domain inlet x = 0 reflects the zero mean velocity of the synthetic jet and therefore a zero mass flux. At a slightly downstream location x = 15, however, the flow does not show a zero mean velocity. Instead, the flow shows a positive, non-zero mean velocity, indicating a net momentum flux in the direction away from the domain inlet. In Fig. 7 it also can be observed that the velocity variation at a downstream location becomes far smaller than that at the domain inlet, which is due to the mixing of the jet with the ambient background fluid. However the period of the velocity oscillation at x = 15 remains the same as the initial periodic variation at the domain inlet at x = 0. This was also shown by the constant distance displayed by the cores of the vortex rings as they moved downstream in Fig. 6.

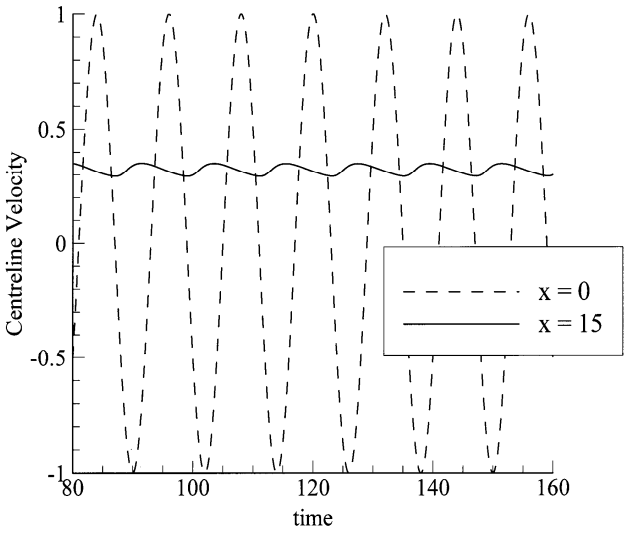

Fig.7 Centreline velocity history of the optimised case at x = 0 and x = 15.

5 Conclusions

The optimisation of various input parameters of an axisymmetric synthetic jet actuator has been carried out, along with an evolution study into the formation of the vortex train associated with synthetic jets. A highly accurate direct numerical simulation based upon the Padé scheme has been used to compute the vortical structures produced due to an oscillating velocity input applied at the jet orifice. Analysis of the mean centreline jet velocity at the orifice compared to data recorded at a downstream location has also shown the development of the positive streamwise momentum flux from the initial zero mean velocity of the jet actuator at the domain inlet.

The results attained have allowed a number of assertions to be made about the input characteristics which yield the optimum streamwise vortex train in terms of vortical strength and longevity.

Throughout the range of physical parameters examined, various vortical structures have been observed in the flow field. The input parameter which was noted to have the greatest effect on jet formation was the actuator oscillation frequency. At low actuation frequencies the vortical structures present in the flow field were noted to be of a larger size; however a true 'vortex train' was not produced as the vortical structures were noted to travel downstream as a lone vortex ring. At high frequencies the jet was noted to be under expanded, in the region near the actuator. In this case vortical structures in the flow field were less coherent and did not persist in the downstream region. As previously stated, this has been determined to be due to re-ingestion of the expelled fluid from the actuator on the subsequent suction stroke. More importantly, the results showed that synthetic jets with zero mean velocity at the inflow behave significantly differently from jets with non-zero mean velocity at the inflow. For a synthetic jet with zero mean velocity at the inlet, the jet developed significant vortical structures at much lower frequencies.

Investigation into the effect of varying the Reynolds number showed the propagation of the vortical structures further downstream with higher Reynolds numbers, as expected.

Analysis of the evolution of the optimised jet case at regular time intervals shows the initial development and propagation of the individual vortex rings which make up the fully developed synthetic jet. The jet can be defined as being fully developed at a time when increasing the overall run time simulation will result in no further downstream propagation of the vortical structures present in the flow. The jet evolution study shows that in this optimised case the jet can be defined as fully developed beyond t = 60. The evolution study also shows the gradual decrease in vortical intensity of each individual vortex pair with time as they move downstream away from the orifice due to mixing of the jet flow with the ambient background fluid.

The centreline velocity of a fully developed synthetic jet shows that a mean positive velocity profile is present at a location downstream of the orifice to which a zero mean velocity profile has been applied. Although the magnitude of the velocity variation is reduced from the initial amplitude of the actuator, a clear non-zero mean velocity is present showing the net momentum flux of the fluid away from the orifice.

The complexity of the overall flow optimisation problem has been reduced by simply simulating the jet orifice as a sinusoidal oscillating velocity input, instead of a full simulation of the entire synthetic jet cavity flow. This initial investigation also uses an idealised axisymmetric configuration in place of a full three-dimensional direct numerical simulation. Due to the nature of the axisymmetric simulation, there is lack of three-dimensional vortex stretching and interaction. This has previously been determined to be due to an inability of an axisymmetric simulation such as this to predict the flow features present due to the small scales. These small scales are of increasing importance in the downstream region, hence the reduction in vortical strength in these regions in this study. However the results attained give a valuable insight into the formation criterion and the evolution of the synthetic jet along with optimal values for the actuator design.

References:

[1] Amitay, D., Pitt, D., Kibens, V., Parekh, D., Glezer, A., *Control of Internal Flow Separation Using Synthetic Jet Actuators*, AIAA 2000-0903, 2000.

[2] Uttukar, Y., Holman, R., Mittal, B. Carroll, M. Sheplak, and L. Cattafesta, *A Jet Formation Criterion for Synthetic Jet Actuators*, AIAA 2003-0636, 2003

[3] Didden, N., On the Formation of Vortex Rings: rolling up and Production of Circulation, *Journal of Applied Mathematics and Physics*, vol. 30, Jan. 1979, pp. 101-116.

[4] Holman, R., Utturkar, Y., Formation Criterion for Synthetic Jets, *AIAA Journal*, Vol. 43, No. 10, 2005, pp. 2110-2116.

[5] Smith, B. L., Glezer, A., Vectoring of adjacent synthetic Jets, *AIAA Journal*, Vol. 43, No. 10. 2005, pp. 2117-2124.

[6] Jiang, X., Zhao, H., Cao, L., Direct computation of a heated axisymmetric pulsating jet, *Numerical heat transfer Part A*, Vol. 46, 2004, pp. 957-979.

[7] Poinsot, T. J., Lele, S. K., Boundary conditions for direct simulation of compressible viscous flows, *Journal of Computational Physics*, Vol. 101, 1992, pp. 104–129.

[8] Dandois, J., Garnier, E., Sagaut, P., Numerical simulation of active separation control by a synthetic jet, *Journal of Fluid Mechanics*, Vol. 574, 2007, pp 25-58

[9] Liang, Y., Taya, M., Kuga, Y., Design of diaphragm actuator based on ferromagnetic shape memory alloy composite, Proc. of *SPIE meeting, Smart Structure and Materials*, San Diego, CA, March, 2003. Vol. 5054-05, 2003